

UC Berkeley

UC Berkeley Previously Published Works

Title

Evaluation of hydrologic components of community land model 4 and bias identification

Permalink

<https://escholarship.org/uc/item/1qg6h8z1>

Authors

Du, Enhao
Di Vittorio, Alan
Collins, William D

Publication Date

2016-06-01

DOI

10.1016/j.jag.2015.03.013

Peer reviewed

1 Evaluation of Hydrologic Components of Community Land Model4
2 and Bias Identification

3 Enhao Du^{1*}, Alan Di Vittorio¹, William D. Collins^{1,2}

4 1. Climate Science Department, Lawrence Berkeley National Laboratory

5 2. Department of Earth and Planetary Science, University of California,
6 Berkeley

7
8 *Corresponding author:

9 Enhao Du

10 Earth Sciences Division

11 Lawrence Berkeley National Laboratory

12 One Cyclotron Road - M/S 74R316C

13 Berkeley, California 94720-8268

14 Phone: +1 805-205-7437

15 Email: enhaodu@gmail.com

16
17 Abstract

18 Runoff and soil moisture are two key components of the global hydrologic cycle
19 that should be validated at local to global scales in Earth System Models (ESMs)
20 used for climate projection. We have evaluated the runoff and surface soil
21 moisture output by the Community Climate System Model (CCSM) along with 8
22 other models from the Coupled Model Intercomparison Project (CMIP5)
23 repository using satellite soil moisture observations and stream gauge corrected
24 runoff products. A series of Community Land Model (CLM) runs forced by
25 reanalysis and coupled model outputs was also performed to identify
26 atmospheric drivers of biases and uncertainties in the CCSM. Results indicate
27 that surface soil moisture simulations tend to be positively biased in high latitude
28 areas by most selected CMIP5 models except CCSM, FGOALS, and BCC, which
29 share similar land surface model code. With the exception of GISS, runoff
30 simulations by all selected CMIP5 models were overestimated in mountain
31 ranges and in most of the Arctic region. In general, positive biases in CCSM soil
32 moisture and runoff due to precipitation input error were offset by negative biases
33 induced by temperature input error. Excluding the impact from atmosphere
34 modeling, the global mean of seasonal surface moisture oscillation was out of
35 phase compared to observations in many years during 1985-2004. The CLM also
36 underestimated runoff in the Amazon, central Africa, and south Asia, where soils

37 all have high clay content. We hypothesize that lack of a macropore flow
38 mechanism is partially responsible for this underestimation. However, runoff was
39 overestimated in the areas covered by volcanic ash soils (i.e. Andisols), which
40 might be associated with poor soil porosity representation in CLM. Our results
41 indicate that CCSM predictability of hydrology could be improved by addressing
42 the compensating errors associated with precipitation and temperature and
43 updating the CLM soil representation.

44 Highlights

- 45 • We evaluated gridded soil moisture and runoff of nine CMIP5 models
- 46 • We isolated biases from the atmosphere model
- 47 • We identified areas with anomalies generated by CLM4
- 48 • We proposed modifications to improve hydrologic simulations in CLM

49

50 Key words

51 CLM4, surface soil moisture, runoff, historical evaluation, bias test

52 1. Introduction

53 The Community Land Model (CLM) serves as the land model for the Community
54 Climate System Model (CCSM) [Collins *et al.*, 2006] and includes land
55 biogeophysics, hydrology, and biogeochemistry. Hydrology comprises key
56 processes that link and integrate atmosphere, ocean, vegetation, and human
57 systems. Increasing greenhouse gas concentrations and potential global
58 warming may affect water cycle dynamics, which in turn provide feedbacks to the
59 atmosphere and land surface. As a tool for predicting future states of ecosystems
60 and climate, land surface model development requires rigorous calibration and
61 validation against observations.

62 The growing demand for assessing the potential impacts of projected climate
63 change on human systems [Field *et al.*, 2014] highlights the importance of
64 understanding surface hydrological responses within fully coupled Earth System
65 Models (ESMs), in addition to evaluating the accuracy of standalone land surface
66 models. While the IPCC AR5 has implemented a new framework for assessing
67 these impacts [Field *et al.*, 2014] a recent study with the newly developed
68 integrated Earth System Model (iESM), which directly couples the Global Change
69 Assessment Model (GCAM) with the Community Earth System Model (CESM)
70 [Collins *et al.*, 2014], has quantified the unintended consequences of not
71 implementing complete consistency among land use and land cover components
72 of the economic Integrated Assessment Models (IAMs) and the biophysical
73 ESMs [Di Vittorio *et al.*, 2014]. The next steps for assessing climate impacts
74 include implementing and examining feedbacks between ESM water supply and
75 IAM water demand and management. In the context of the iESM, closer
76 examination of the surface hydrology of the fully coupled CCSM/CESM will
77 enable development of a more consistent framework for incorporating human-
78 earth water cycle feedbacks into projections of water availability and use.

79 Runoff is an important component of the hydrological cycle, but runoff trend
80 detection at the global scale is a difficult task. Even the sign of the trends are
81 uncertain, as recent estimates of global runoff trends in the twentieth century
82 from various modeling studies are both positive [Gedney *et al.*, 2006; Labat *et al.*,
83 2004; Piao *et al.*, 2007] and negative [Dai *et al.*, 2009; Shi *et al.*, 2011]. Positive
84 trends may be a result of increased continental precipitation, stomatal closure
85 due to rising CO₂ concentration, land use changes, or decline of land ice content
86 [Alkama *et al.*, 2013]. Decreasing trends in global runoff could be a consequence
87 of climate forcing changes with minor effects from nitrogen deposition and land
88 use change [Shi *et al.*, 2011]. These uncertainties in runoff simulations are
89 largely due to different model implementations of atmosphere-plant-soil system

90 interactions and the range in responses from these parameterizations to model-
91 specific climate forcings.

92 Soil moisture has been demonstrated to affect regional climate via evaporation
93 and evaporative cooling [Seneviratne *et al.*, 2013]. For example, atmospheric
94 circulation over the land surface is largely affected by soil moisture during
95 summer [Owe *et al.*, 2008]. In particular, surface soil moisture controls
96 partitioning between sensible and latent heat, and affects partitioning between
97 overland flow and infiltration [Hou *et al.*, 2012]. However, surface soil moisture is
98 among the most complex hydrologic variables to simulate as it interacts with the
99 atmosphere, plant canopy and roots, and vadose zone. This complexity is likely
100 evidenced by studies showing that peak variability in soil moisture occurs at the
101 surface [Decker and Zeng, 2009].

102 Our evaluation procedures comply with the benchmarking framework proposed
103 by Luo *et al.* [2012]. We focus on runoff and soil moisture because observation-
104 based, gridded, global datasets have recently become available for these two
105 key hydrologic variables [Fekete and Vorosmarty, 2002; Liu *et al.*, 2012]. Other
106 variables such as river discharge and soil water storage of CLM4 [Lawrence *et al.*,
107 2011] and earlier versions (3-3.5) were reported to match observations of
108 major basins globally, although the accuracy of timing for simulated hydrologic
109 quantities varied among rivers and areas [Lawrence *et al.*, 2011; Oleson *et al.*,
110 2008; Qian *et al.*, 2006]. However, CLM4 hydrologic simulations have not been
111 fully assessed at the level of a global grid. Thus, we define a set of metrics
112 including absolute and normalized biases, temporal correlation, and seasonal
113 dynamics to identify model strengths and deficiencies at the grid level. Using
114 these metrics, we identify the contributions of uncertainty from both the
115 atmosphere and the land components of the earth system model to soil moisture
116 and runoff. Based on our evaluation, we propose improvements to the land
117 model hydrology. Our results not only meet evaluation objectives that are
118 coincident with CMIP5 goals [Taylor *et al.*, 2012], they also provide insights
119 toward coupling ESM and IAM water cycles to examine human-earth feedbacks
120 affecting water supply, demand, and management.

121

122 **2. Datasets and methods**

123 The study was designed as two parts to answer following questions:

- 124 1. How well do the fully coupled models, particularly CCSM/CLM, represent
125 the surface soil moisture and runoff? What atmospheric forcings have the
126 greatest influence on these two variables?

127 The hydrologic simulations of the CMIP5 models are largely dependent on the
128 forcings of various atmosphere models, but the ensemble comparison may
129 still help to reveal areas where hydrology is frequently underrepresented by
130 the earth system models and areas where observations/satellite products
131 have biases.

132 2. What are the contributions of these dominant forcings to hydrologic biases?
133 How do these biases relate to biases generated by land component?
134 What are the potential modifications for addressing land component –
135 driven biases?

136 By applying alternate atmospheric forcings, offline CLM simulations help to
137 determine contributions of biases in the coupled model from those driven by
138 the land model component.

139 *2.1 Fully coupled global model outputs*

140 The CCSM version 4.0 (CCSM4) is a coupled climate model for simulating the
141 earth system. The historical model outputs are available from the Climate Model
142 Intercomparison Project Phase 5 (CMIP5) repository. We use outputs from the
143 CCSM4 MOther of All Runs (MOAR) for several reasons. First, MOAR is the
144 historical control run with fixed satellite phenology and hence more realistic
145 interactions between vegetation and hydrological processes than the
146 unconstrained model. This constraint helps us focus on the physical rather than
147 vegetative hydrologic components of version 4 of the land model (CLM4) in
148 CCSM4. The MOAR run is the only century-long ensemble member with sub-
149 daily atmosphere variables, making it possible to perform subsequent offline runs
150 driven by the same set of forcing. Also, the MOAR outputs cover the time period
151 of 1850-2005 that is overlapped with observations.

152 In CLM4, soil moisture dynamics is controlled by infiltration, runoff (surface and
153 subsurface), gradient diffusion, gravity, and root extraction in a ten-layer model
154 (3.8 m) plus an underlying five-layer aquifer (5 m). The runoff is parameterized as
155 exponential functions of groundwater level [Oleson *et al.*, 2010]. The model has
156 been calibrated and validated against major river discharge and terrestrial water
157 storage observations [Oleson *et al.*, 2008]. Using uncertainty quantification
158 framework, Huang *et al.* [2013] found that subsurface runoff generation and soil
159 texture-related parameters are the most significant to runoff simulations. Details
160 of hydrologic parameterizations in CLM4 can be found in [Huang *et al.*, 2013; Niu
161 *et al.*, 2005; Niu *et al.*, 2007; Oleson *et al.*, 2008]. The choice of CLM4 hydrologic
162 parameters may have considerable impact on the results of runoff and soil
163 moisture, but is not the scope of the study.

164 We included eight other models from the CMIP5 repository in our comparison
165 with observations: HadCM3, MIROC5, GFDL-CM3, CSIRO-Mk3, BCC-csm1,
166 MRI-ESM1, FGOALS-g2, and GISS-E2-R. The models were selected to meet
167 two criteria: they must have both runoff and surface soil moisture monthly outputs
168 and they must have historical runs. Brief descriptions of each model and
169 institution can be found in CMIP5 website ([http://cmip-
170 pcmdi.llnl.gov/cmip5/availability.html](http://cmip-pcmdi.llnl.gov/cmip5/availability.html)). Outputs were extracted from a single
171 historical run (1850-2005) by each model.

172 Two types of coupled model output were involved in this evaluation: the
173 hydrologic outputs (i.e. runoff and surface soil moisture) for comparison against
174 observations, and the atmosphere outputs from CCSM4 MOAR simulations for
175 driving the CLM4 offline runs. We extracted monthly surface soil moisture in the
176 top 10 cm and runoff from the CMIP5 archive via the Earth System Grid
177 (<http://pcmdi9.llnl.gov>) for the CCSM4 and the eight other models. Coupled
178 model monthly land outputs were extracted from ensemble member r6i1p1 for
179 CCSM4 and from r1i1p1 for the eight other models. Atmosphere outputs from the
180 coupled CCSM MOAR run were acquired from the National Center for
181 Atmosphere Research (NCAR) via the Earth System Grid
182 (<https://www.earthsystemgrid.org>) and used to force the offline CLM4 runs. The
183 forcing data include 3-hourly solar radiation, specific humidity, temperature,
184 surface pressure, and wind together with 6-hourly fields of precipitation.

185 *2.2 Observational data*

186 *2.2.1 Surface soil moisture*

187 Soil moisture products have been estimated from an individual remote sensing
188 satellite in various studies (e.g., *Al-Yaari et al.* [2014] and *Loew et al.* [2013]), but
189 a multi-sensor approach has improved global soil moisture estimates. *Liu et al.*
190 [2012] have merged four passive microwave soil moisture retrievals from the
191 Scanning Multichannel Microwave Radiometer, the Special Sensor Microwave
192 Imager, the Tropical Rainfall Measuring Mission microwave imager, and the
193 Advanced Microwave Scanning Radiometer – Earth Observing System with two
194 active microwave soil moisture estimates from the European Remote Sensing
195 satellite and the Advanced Scatterometer into the new European Space Agency
196 (ESA) global soil moisture product. The product's temporal domain ranges from
197 1978 to 2010 with daily values at 0.25° spatial resolution. The detection depth of
198 the microwave signal ranges from 2 to 5 cm depending on the type of sensor and
199 soil condition [*Liu et al.*, 2012]. We use Volumetric Water Content (VWC, vol vol⁻¹)
200 as the basis for our comparisons.

201 The ESA data product has no coverage in densely vegetated regions such as the
202 Amazon and central Africa where dense canopy masks out both passive and
203 active microwave signals. The soil moisture retrievals are also absent under
204 frozen or snow conditions. Whenever data are available, the areas are included
205 in the calculation as well as the model simulations. Intercomparison and
206 validation of the microwave satellite data have been conducted at regional and
207 continental scales against in-situ observations [Albergel *et al.*, 2012; Brocca *et al.*,
208 2011; Gruhier *et al.*, 2010; Loew *et al.*, 2013]. In general the satellite product
209 accurately reproduces the seasonal cycle as well as short-term variability.

210 2.2.2 Monthly runoff

211 The University of New Hampshire (UNH) Global Runoff Data Center (GRDC
212 hereafter) composite runoff field V10 is a gridded runoff dataset at 0.5 degree
213 [Fekete and Vorosmarty, 2002]. The dataset was constructed by first calculating
214 basin-scale runoff based on a water balance model developed by UNH. The
215 water balance model (WBM) simulation at each cell was corrected by runoff
216 estimates for the corresponding interstation area. The interstation areas were
217 defined by a river routing model, the Global Simulated Topological model, to
218 which the GRDC stations were geo-registered. A total of 663 GRDC stations
219 were included and represented 72% of actively discharging areas. The majority
220 of discharge records were from the 1970s and the final product is a composite
221 annual runoff. The WBM-modeled runoff from 1971 to 1980 was averaged to
222 approximate the time period.

223 The runoff dataset has more complete global coverage than the soil moisture
224 dataset, enabling evaluation of densely forested areas such as the Amazon and
225 central Africa and permafrost areas such the Himalayas and Arctic Circle. We
226 compared the runoff differences divided by Global Precipitation Climatology
227 Centre (GPCC) precipitation reanalysis, which gives the normalized runoff
228 difference (NRD):

$$NRD = \frac{Q_{model} - Q_{obs}}{P}$$

229 where Q_{model} and Q_{obs} denote the modeled and observed runoff and P the GPCC
230 precipitation. NRD was used instead of percent change because the long-term
231 runoff is zero or close to zero in arid areas, making any percent difference either
232 very large or infinite. We applied GPCC precipitation instead of precipitation from
233 each corresponding model because our aim was to reduce the range of runoff
234 difference induced by variations in modeled precipitation. Dividing runoff by
235 precipitation within each model generates a runoff ratio that describes the portion

236 of runoff relative to precipitation, which is not the intention of this comparison.
 237 Furthermore, applying precipitation from each individual model also introduces
 238 uncertainties from atmospheric simulation that we wanted to minimize in our
 239 comparison. The GPCC monthly precipitation 1-degree data [Schneider *et al.*,
 240 2011] were provided by the NOAA/OAR/ESRL Physical Science Division from
 241 the website at <http://www.esrl.noaa.gov/psd>.

242 2.2.3 Qian’s reanalysis data and GPCC

243 *Qian et al.* [2006] adjusted NCEP-NCAR (National Centers for Environmental
 244 Prediction-National Center for Atmospheric Research) reanalysis forcing dataset
 245 by combining it with station records and satellite observations of temperature,
 246 precipitation, and cloud cover. Qian’s reanalysis dataset covers the global land
 247 areas with 3-hourly and T62 (~1.875°) resolution and serves as the offline CLM
 248 model forcing data from 1948 to 2004.

249 The GPCC full data reanalysis version 6.0 comprises globally gridded gauge-
 250 analysis precipitation products over land areas derived from quality controlled
 251 station data [Becker *et al.*, 2013]. The monthly precipitation data were used to
 252 normalize the runoff discrepancies between CMIP5 models and observations.

253 2.3 Offline experiments to assess sources of error

254 We extracted climate variables from the MOAR run to construct the forcings for
 255 offline CLM4 runs. The MOAR climate variables are available in 3-hourly, 6-
 256 hourly, and monthly time steps. All our processing was based on 3-hourly data.
 257 The standard climate forcings for a CLM4 historical run with satellite phenology
 258 include three NetCDF files: 3-hourly solar radiation, 6-hourly precipitation
 259 (converted by averaging from 3-hourly), and 3-hourly surface temperature,
 260 specific humidity, pressure, wind speed. The MOAR climate variables were
 261 combined with Qian’s reanalysis data [Qian *et al.*, 2006] to construct offline runs

262 with four sources of climate forcings (Table 1):

263 Table 1. List of offline experiments and forcings

	QIAN	MOAR	MOAR_PRECIP	MOAR_TEMP
Precipitation	reanalysis ¹	coupled run ²	reanalysis	coupled run
Temperature/humidity	reanalysis	coupled run	coupled run	reanalysis
Other forcings ³	reanalysis	coupled run	coupled run	coupled run

264 1. Qian’s 2006 reanalysis dataset (see section 2.2.3)

265 2. atmosphere forcings from MOAR coupled run

266 3. other forcings include solar radiation, wind, and surface pressure

267

- 268 a. Qian's 2006 reanalysis dataset (QIAN hereafter)
- 269 b. Atmosphere outputs from the MOAR coupled run (MOAR hereafter)
- 270 c. Qian's reanalysis, but with precipitation data from the MOAR run
- 271 (MOAR_PRECIP hereafter)
- 272 d. Qian's reanalysis, but with surface temperature and specific humidity from
- 273 MOAR run (MOAR_TEMP hereafter).

274

275 In the offline experiments, soil moisture is extracted from top 4.5 cm soils and
276 excludes ice content. This soil moisture output matches the satellite product
277 closely both in scale and phase, and therefore provides the most appropriate
278 comparison with observation datasets. Monthly global mean values were
279 compared between simulations and observations to reveal the dynamics of runoff
280 and soil moisture. Differences between MOAR_TEMP and MOAR_PRECIP
281 relative to QIAN determine what fractions of the total variance between MOAR
282 and QIAN are due to temperature/humidity and precipitation, respectively.

283 *2.4 Correlation analyses*

284 Temporal correlation analysis between model simulations and observations used
285 Pearson's correlation coefficient r . The Pearson correlation coefficient was
286 calculated between simulations and observations, and between the hydrologic
287 variables (runoff and surface soil moisture) and atmosphere forcings
288 (precipitation and surface temperature).

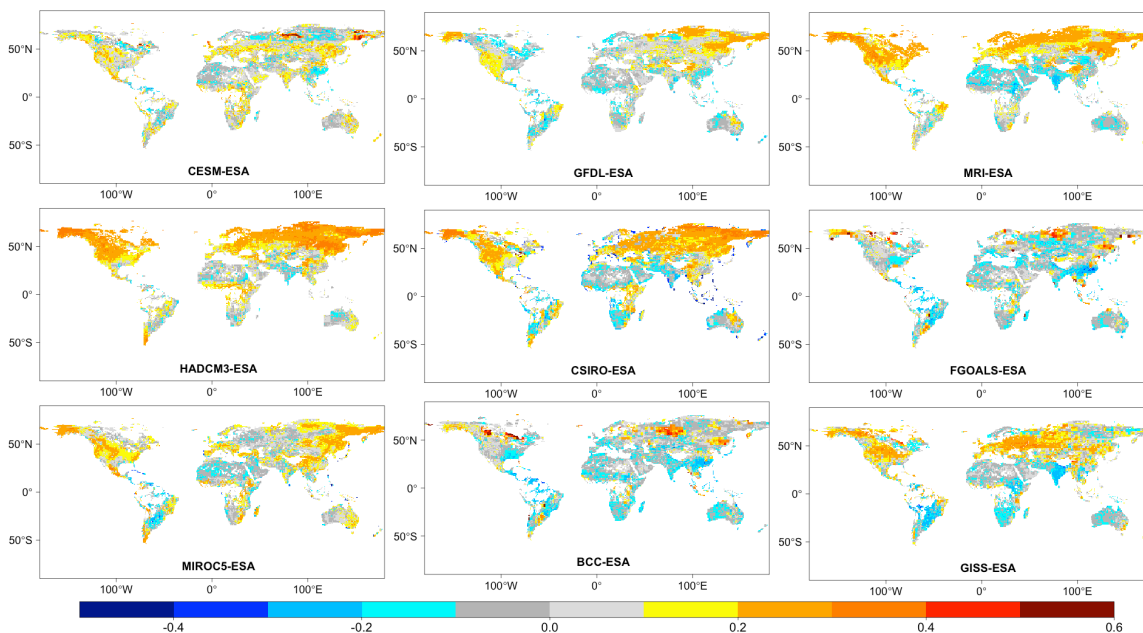
289

290 **3. Results and discussions**

291 *3.1 Surface soil moisture*

292 The soil volumetric water content differences between CCSM4 and the ESA
293 dataset indicate that soil moisture discrepancies are within 5% in the majority of
294 the area covered by the ESA dataset. The inclusion of wetland areas in the
295 surface soil moisture data in the CCSM4 CMIP5-archived outputs contributes to
296 the apparent, but incorrect, signal of permanently saturated soils in high latitude
297 areas between 50 to 70° N including the Hudson Bay in Canada and parts of
298 Siberia (Figure 1). For this reason, the wetland areas have been omitted from the
299 calculation of surface soil moisture in the remainder of our analyses. Outside of
300 the wetland areas, CCSM4's soil moisture exceeded ESA's observation by 0.05-
301 0.20 VWC in predominantly mountainous regions covering the Rocky Mountains,

302 central Europe and the Alps, central Africa, areas immediately south of
 303 Himalayas including India, Bangladesh, Burma etc., northern and central China,
 304 and western Australia. CCSM4 underestimated surface soil moisture by up to
 305 0.20 in high latitude areas of North America and Eurasia, central Asia, and
 306 southern China.



307
 308 Figure 1. Absolute surface soil moisture difference indicates CCSM4's soil moisture
 309 exceeds ESA's observation by up 0.05-0.20 (vol vol⁻¹) in the Rocky Mountains, central
 310 Europe, central Africa, south of Himalayas, most of China, and west Australia. CCSM4
 311 underestimated surface soil moisture by up to 0.20 in high latitude areas. Most other
 312 CMIP5 models had positive biases in high latitude areas and United States except
 313 FGOALS and BCC.

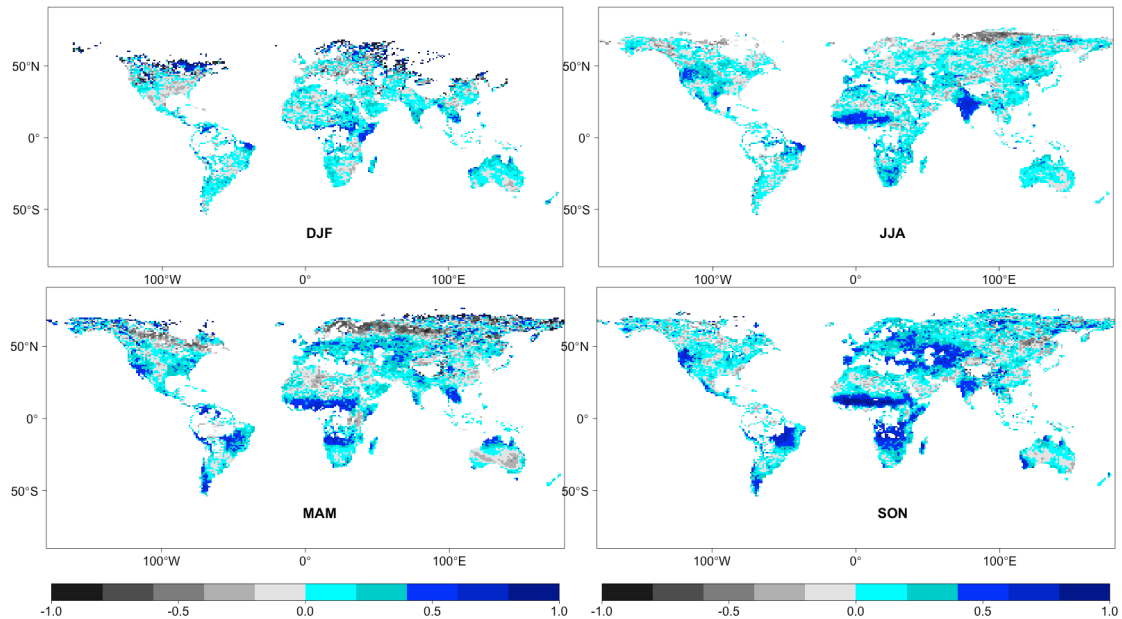
314 In contrast, with the exception of FGOALS and BCC, most other CMIP5 models
 315 had positive biases in high latitude areas and in the United States. Both FGOALS
 316 and BCC models suffered from the inclusion of wetland in the soil moisture
 317 calculation and thus displayed oversaturation. This is not surprising because
 318 FGOALS used an earlier version of the CCSM land surface model (CLM3).
 319 FGOALS and BCC were the only models with an overall negative bias compared
 320 to ESA dataset. An extremely dry bias followed the edge of continents and small
 321 islands in CSIRO.

322 Two types of mismatch between these simulation outputs and satellite
 323 observations cause models to overestimate soil moisture. The first possible
 324 cause is a depth mismatch between the archived top 10 cm layer and the 2-5 cm
 325 layer measured by the instruments in the ESA data set. Although *Wagner et al.*

326 [1999] has demonstrated that surface soil moisture can act as a predictor of
327 deeper soil profile, the surface soil is inherently drier than the underlying layers at
328 long time scales (e.g. monthly) because of loss by surface evaporation. The
329 archived outputs include more than double the depth of the satellite observation,
330 which potentially introduces a positive bias in water content in many areas with
331 respect to the ESA product. The second possible cause is a phase mismatch
332 between the modeled and observed VWC. The archived surface soil water
333 content includes the mass of water in all phases, whereas the satellite data
334 includes only the liquid phase of soil water. The satellite data as a rule excludes
335 areas with snow cover or land surface temperature below zero, but it may not
336 exclude all areas with ice content below the surface that would not be detected
337 as water content. Therefore the satellite product is potentially 'drier' than the
338 modeled soil, especially in high latitude areas.

339 Therefore both thicker depth and the inclusion of ice content in the CCSM4
340 simulation tend to give higher water content values than the ESA observations. In
341 general the two types of mismatch would artificially shift the systematical bias in
342 modeled surface soil moisture toward small positive values. For the purposes of
343 this comparison, areas with a negative difference or a positive difference greater
344 than 0.2 exhibit significant surface soil moisture biases. Fortunately, we were
345 able to remove these mismatches from our offline analyses because we ran our
346 own simulations and were not restricted to archived data. On the other hand,
347 under certain extreme circumstances, the modeled and satellite-derived
348 estimates of a given soil could differ by the total soil pore volume. This situation
349 would occur only where the surface temperature is above freezing so that the
350 measurement is included in the data set but the ground remains partially to
351 completely frozen, thereby resulting in a spurious satellite retrieval of low VWC
352 while the model output may contain a frozen, saturated soil column.

353 The evaluation of soil moisture estimation may be limited by the quality of the
354 observational dataset. ESA soil moisture products were found to have poor
355 correlations at high latitude of north hemisphere against the reanalysis of the
356 European Centre for Medium-Range Weather Forecasts Interim [Albergel *et al.*,
357 2013], partly owing to the low average observation densities in northern latitudes
358 due to snow and ice [Dorigo *et al.*, 2014]. Also, the quality of ESA soil moisture
359 dataset is affected by surface soil moisture simulation of GLDAS-1 Noah, a land
360 surface model that was used to rescale the microwave products [Liu *et al.*, 2012].



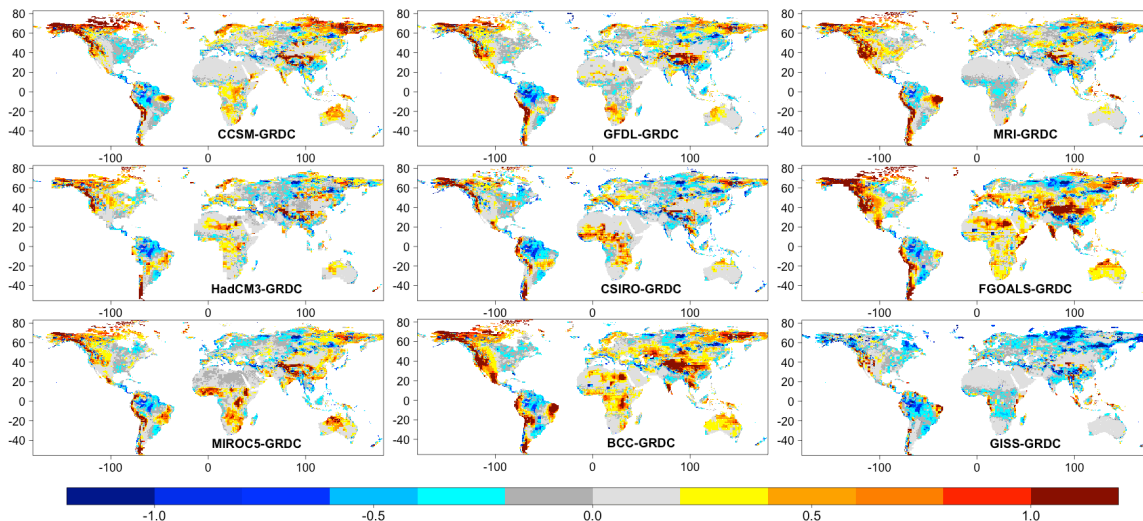
361
 362 Figure 2. Temporal correlation of CCSM4's surface soil moisture in four seasons
 363 indicates monthly soil moisture dynamics are better correlated with observations in low-
 364 to mid-latitude areas.

365 The temporal dynamics of soil moisture, however, are more consistent than the
 366 magnitudes between the models and observations (Figure 2). Monthly CCSM4
 367 soil moisture dynamics are better correlated with observation in tropical areas,
 368 but have decreased coefficients in high latitude areas, especially in northern
 369 hemisphere winter (DJF) and spring (MAM). Similar to CCSM4, most CMIP5
 370 models displayed similar annual spatial patterns with decreased correlation
 371 coefficient in permafrost areas such as Canada and Siberia and in arid zones
 372 such as the Sahara and central Australia (not shown). The high latitude areas
 373 with the least correlation generally have the largest absolute biases. Overall, soil
 374 moisture is better correlated in northern hemisphere summer and fall, but has
 375 more negative coefficients in spring (MAM), implying model deficiency in
 376 snowmelt simulation.

377 3.2 Runoff

378 Canada and Siberia and the major mountain ranges, including the Rocky
 379 Mountains, Andes, and Himalayas are the areas where most models
 380 overestimate runoff by more than the magnitude of the Global Precipitation
 381 Climatology Centre (GPCC) precipitation reanalysis (Figure 3). FGOALS and
 382 BCC both produce unrealistically high amounts of runoff in the Saharan region.
 383 GISS is the exception in that it generally underestimates runoff. The Amazon is
 384 the only region where all models underestimate runoff, and these results are
 385 consistent with a negative precipitation bias reported for CMIP5 models [Mehran

386 *et al.*, 2014]. Similar to soil moisture, the runoff comparison has a mismatch
 387 between the simulation and observations: the CMIP5 models define runoff as the
 388 total liquid water leaving the grid cell, which accounts for both surface and
 389 subsurface terms, while the GRDC runoff product assumes all water leaving a
 390 grid cell emerges as river discharge at a given stream gauge. Thus, the GRDC
 391 product may underestimate total runoff in headwater and upstream basins if
 392 subsurface water does not discharge within a grid cell and/or discharges to a
 393 stream outside a measurement basin.



394

395 Figure 3. Precipitation normalized runoff difference between CMIP5 models and GRDC
 396 dataset. Most CMIP5 models, except GISS, produced higher runoff than GRDC in
 397 mountain ranges. All models underestimated runoff in the Amazon.

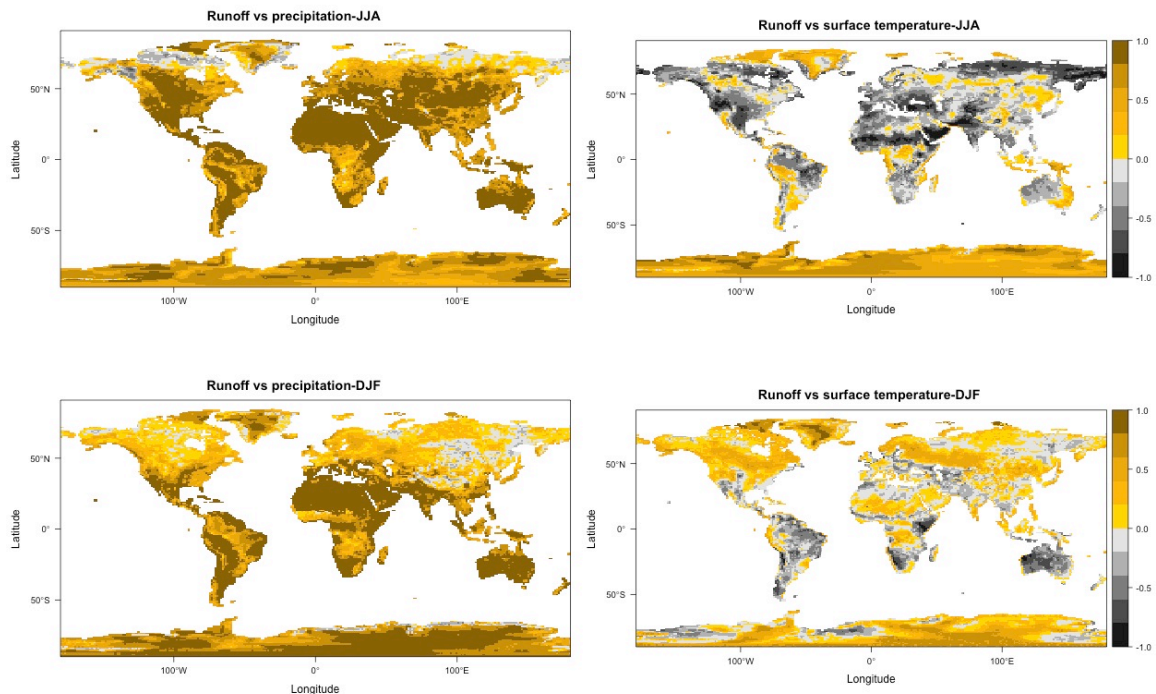
398 Our evaluations of both surface soil moisture and runoff indicated that the largest
 399 discrepancies between model outputs and observations occur in mountainous
 400 and high latitude areas. *Mehran et al.* [2014] found that CMIP5 models generally
 401 overestimate precipitation in steep terrain. Their bias map for CESM1_BGC_es,
 402 a version close to CCSM4, shows a very similar pattern to the runoff bias in this
 403 study except in Canada and Siberia. We speculate that that the runoff biases in
 404 mountainous regions are caused by precipitation biases in the atmosphere model,
 405 while biases in high latitude areas may be caused by other atmosphere forcings
 406 or by the land surface model algorithms.

407 Another potential reason for most CMIP5 models having large biases in
 408 mountainous areas may be tracked to deficiencies in the GRDC dataset. The
 409 gridded GRDC runoff was generated by linking discharge gauging station data
 410 with a digital river network and distributing runoff across interstation regions
 411 using a water balance model. The WBM itself could be biased due to
 412 meteorological forcings (e.g. precipitation) and physical (e.g. soil properties) or

413 biophysical attributes (e.g. land cover). Inconsistencies also exist between the
414 GRDC station data and the river network due to resolution discrepancies and
415 data quality [Fekete and Vorosmarty, 2002], but the GRDC dataset is still the
416 only gridded runoff field available for global scale evaluation. The GRDC
417 composite runoff dataset provides only a monthly mean runoff field, which limits
418 our analysis to bias evaluation.

419 3.3 Atmosphere-land hydrology correlations in the coupled CCSM4

420 Four potential sources of bias are 1) the error from observational data, 2)
421 structural deficiencies of CLM4, 3) forcing errors from the atmosphere, and 4)
422 model parameterization. Many researchers are currently working to improve CLM
423 and its parameters, and here we attempt to identify the effects of atmospheric
424 forcing on land hydrology to better understand CLM deficiencies.



425

426 Figure 4. Correlation between runoff and precipitation, and runoff and surface
427 temperature in winter and summer, respectively. Precipitation is positively correlated to
428 runoff in northern hemisphere summer (JJA) except for the areas above Arctic Circle. In
429 northern hemisphere winter (DJF), the correlation is weakened in the high elevation
430 areas where freeze and thaw dominate the hydrology. Surface temperature is negatively
431 correlated to runoff in JJA but more positively correlated in DJF. Correlations with soil
432 moisture follow similar patterns.

433 Atmospheric forcings are expected to be one of the major sources of bias in land
434 surface hydrology when hydrologic cycles are driven by climate model outputs.
435 Precipitation has been found to largely affect runoff trends while temperature has
436 relatively weaker influences [Gerten *et al.*, 2008; McCabe and Wolock, 2011].
437 CLM4 imports six atmospheric variables from the Community Atmosphere Model
438 4.0 (CAM4) including solar radiation, precipitation, surface temperature, pressure,
439 wind, and specific humidity. Monthly correlation analysis reveals that precipitation
440 and surface temperature are the major predictors for soil moisture and runoff.
441 The correlations for each hydrologic variable exhibit similar geographic and
442 temporal patterns. In northern hemisphere summer (JJA), precipitation is
443 positively correlated to both runoff (Figure 4) and soil moisture (not shown),
444 except for areas above Arctic Circle. In northern hemisphere winter (DJF),
445 precipitation is not as strongly correlated to runoff and soil moisture, especially in
446 the northern hemisphere and in high elevation areas when freeze and thaw are
447 the main drivers for hydrology. Surface temperature, on the other hand, is
448 negatively correlated to soil moisture and runoff in JJA as high temperature dries
449 up soil via evaporation and transpiration. Areas where temperature correlation
450 coefficients are positive are either within the Arctic Circle or affected by summer
451 monsoon. In DJF high temperatures induce snow thaws that consequently
452 moisten the soil, therefore surface temperature is more positively correlated to
453 the two hydrologic components. The rest of the atmospheric forcings indicate
454 much weaker correlations with the two hydrologic variables.

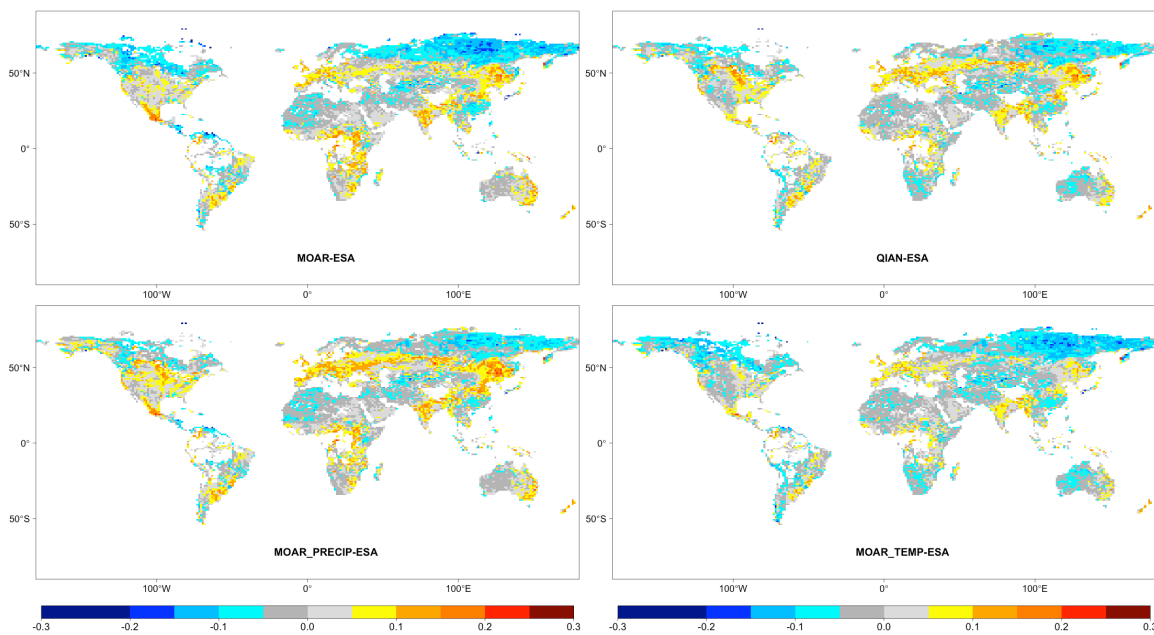
455 As the precipitation shows strong correlation to the runoff and surface soil
456 moisture in mid- to low-latitude areas and temperature shows stronger (positive
457 and negative) correlation in high latitude zones, understanding the geographic
458 differences in atmosphere-driven biases can help evaluation of hydrological
459 processes in the land surface model. For example, the CMIP5 archived models
460 often have larger biases in high latitude areas where snow and permafrost
461 freeze-and-thaw mechanism may be underrepresented due to deficiency from
462 temperature or land model. Similarly, runoff simulation of CMIP5 models in high
463 latitude areas may be more biased by temperature forcing, but more affected by
464 precipitation in mountainous areas. The correlations between climate forcings
465 and hydrologic variables open the possibility of isolating the biases from
466 atmospheric forcings therefore revealing respective sources of uncertainty from
467 the atmosphere and land models.

468 *3.4 Atmospheric drivers of soil moisture and runoff errors in CLM4*

469 The offline MOAR simulation demonstrates that our offline runs can be used to
470 diagnose the coupled model simulations (i.e. CMIP5). The offline MOAR
471 simulation generates almost identical 10-cm soil moisture (comparisons not

472 shown here) and surface runoff as the coupled simulation, except where the
 473 wetland area has been removed from the soil moisture calculations in the offline
 474 outputs. See section 3.1 for discussion of improperly inclusion of wetland in soil
 475 moisture outputs in CMIP5 simulations. This confirms that offline runs can be
 476 used to determine the error sources of the land model hydrology in the coupled
 477 model.

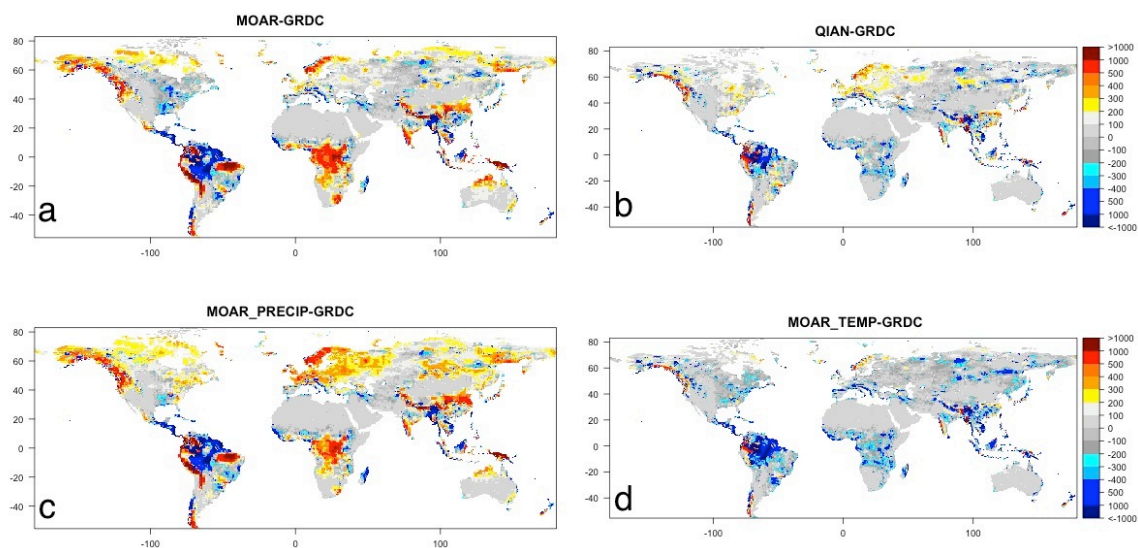
478 To better evaluate the contributions of atmospheric forcing error to hydrologic
 479 uncertainty, the following analyses reduce the effects of soil depth and ice
 480 content mismatch present in the CMIP5 analysis of soil moisture. For the offline
 481 analyses, we used the modeled soil moisture in the top 4.5 cm layers, which
 482 matches closely with the satellite detecting depth, and included only liquid water
 483 in the modeled water content. These procedures were not possible for the CMIP5
 484 evaluations as the CMIP5 repository provides limited output variables. The
 485 difference between the two outputs is mostly within 0.04 except the CMIP5 soil
 486 (10 cm with ice content) contains 0.1-0.2 more water content in high latitude areas.
 487 This explains the discrepancies in high latitude areas between two comparisons
 488 of coupled and offline runs (Figure 1, CCSM-ESA vs Figure 5, MOAR-ESA).



489

490 Figure 5. Absolute biases between offline runs and ESA surface soil moisture
 491 observations. a). the offline MOAR run resembled the CCSM4 coupled run. b). Qian's
 492 reanalysis forced run served as the reference that alleviated the underestimation of soil
 493 moisture in high latitude areas and Central America. c). offline run forced by reanalysis
 494 and modeled precipitation increased soil moisture compared to MOAR and QIAN runs,
 495 especially in the band of north 40 to 70. d) offline run forced by modeled temperature
 496 and relatively humidity reduce surface soil moisture compared to other offline runs.

497 Qian's reanalysis dataset is the closest atmosphere forcings to the observations
 498 and was therefore intended to isolate the biases to the land surface model only.
 499 Using reanalysis forcings improved soil moisture and runoff outputs with respect
 500 to the offline MOAR simulation. Underestimation of soil moisture in the MOAR
 501 simulation was alleviated in the QIAN simulation in high latitude areas and
 502 Central America (Figure 5). Additionally, positive differences from ESA data in
 503 Europe and Africa were reduced in the QIAN simulation. Runoff output was even
 504 more drastically improved in the QIAN simulation. The overestimation of runoff in
 505 mountains was mostly alleviated (Figure 6a and b), including the Rocky
 506 Mountains, Andes, Himalayas, and Northern Oceania. The QIAN simulation also
 507 improved runoff in the eastern Amazon, central Africa, and high latitude areas,
 508 although it increased overestimation in Eastern Europe. East of the Amazon and
 509 Central Africa changed from positive biases to neutral or negative. Overall, the
 510 biases in mountainous and tropical areas have been improved by using
 511 reanalysis data in place of the MOAR atmosphere model outputs.



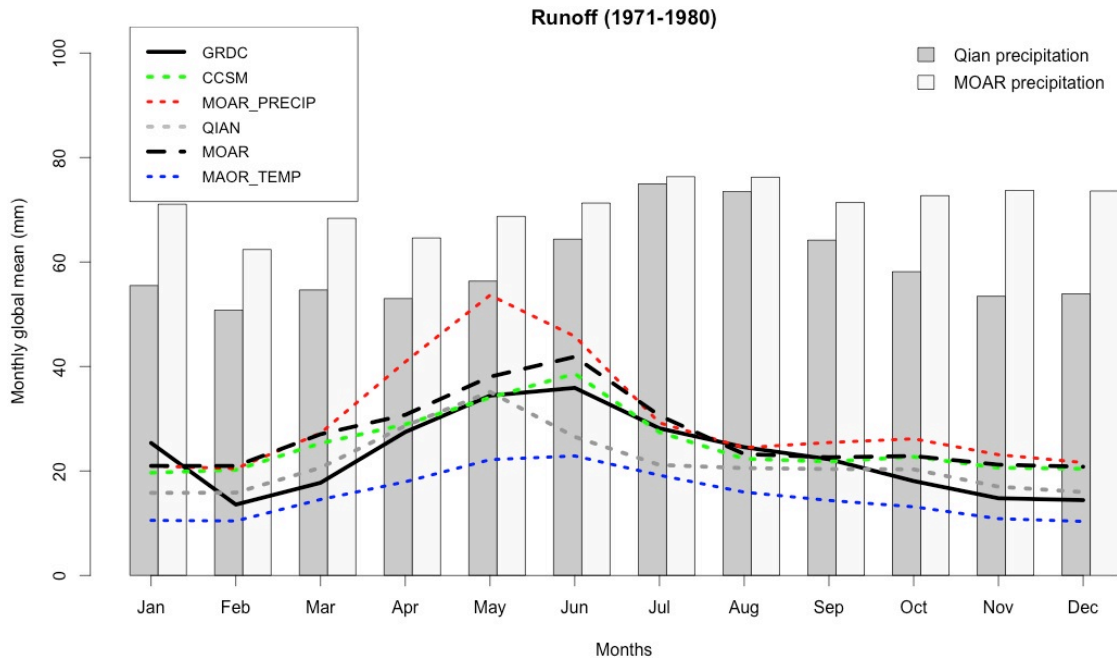
512

513 Figure 6. Absolute biases between offline runs and GRDC runoff dataset. Similar as
 514 surface soil moisture, a) offline run driven by modeled forcings; b) offline run driven by
 515 reanalysis eliminated most of positive biased in mountainous areas; c) offline run driven
 516 by MOAR precipitation produced more positive biases than the reference; d) offline run
 517 driven by modeled temperature and relative humidity changed the overall positive biases
 518 into negative.

519 Independent use of modeled precipitation and temperature forcings for offline
 520 simulations indicates that these atmospheric inputs have opposing effects on
 521 land surface hydrology with respect to their respective reanalysis forcings. The
 522 MOAR_PRECIP simulation increases soil moisture compared to the QIAN

523 simulation, especially within the latitude band of north 40° to 70°, but otherwise
524 has limited effects across the rest of the land surface (Figure 5b and c). The
525 MOAR_PRECIP simulation has a greater impact on runoff through increases in
526 area and magnitude of positive biases (Figure 6b and c). Furthermore, the soil
527 moisture and runoff in the MOAR_PRECIP simulation are greater than in the
528 MOAR simulation (Figures 5a and c, and 6a and c). The MOAR_TEMP
529 simulation shows that modeled temperature and humidity reduced the surface
530 moisture and runoff with respect to the QIAN simulation (Figures 5b and d, and
531 6b and d). The runoff bias maps in particular show the distinct contrast between
532 runs driven by modeled precipitation and temperature (Figure 6c and d). In the
533 original coupled CCSM4 and offline MOAR simulations the positive bias
534 introduced by precipitation input is canceled out to varying degrees around the
535 globe by the negative bias from temperature input.

536 Monthly global 10-year mean runoff (1971-1980) shows a similar pattern of
537 opposing hydrological effects of modeled precipitation and temperature inputs.
538 The CMIP5 fully coupled CCSM4 simulation matches observations well in April to
539 September when hydrologic cycles are active (Figure 7). The QIAN simulation
540 matches observations even better at low flow months, but underestimates runoff
541 in June and July. This indicates that either the Qian dataset has low precipitation
542 or high temperature bias in these two months, or the CLM has deficiency in
543 simulating the drying limb of the spring peakflow. The offline MOAR simulation
544 follows the coupled run well with subtle discrepancies in spring and summer.
545 These discrepancies are likely induced by lack of land-atmosphere feedbacks
546 (e.g. evapotranspiration effects on temperature and humidity). The
547 MOAR_PRECIP simulation has high positive bias in spring and early summer
548 (February to June in northern hemisphere, September to December in the
549 southern hemisphere) when snow melts and high flows occur. These are the
550 months when MOAR precipitation is more positively biased than QIAN, implying
551 precipitation is the main driver of runoff bias. In contrast, the MOAR_TEMP
552 simulation has the greatest negative bias compared to the other three
553 simulations throughout the year. Peakflow timings were advanced from June to
554 May in the QIAN and MOAR_PRECIP simulations. These monthly global results
555 are consistent with the spatial results in that opposite hydrological effects of
556 modeled precipitation and temperature inputs cancel each other out.

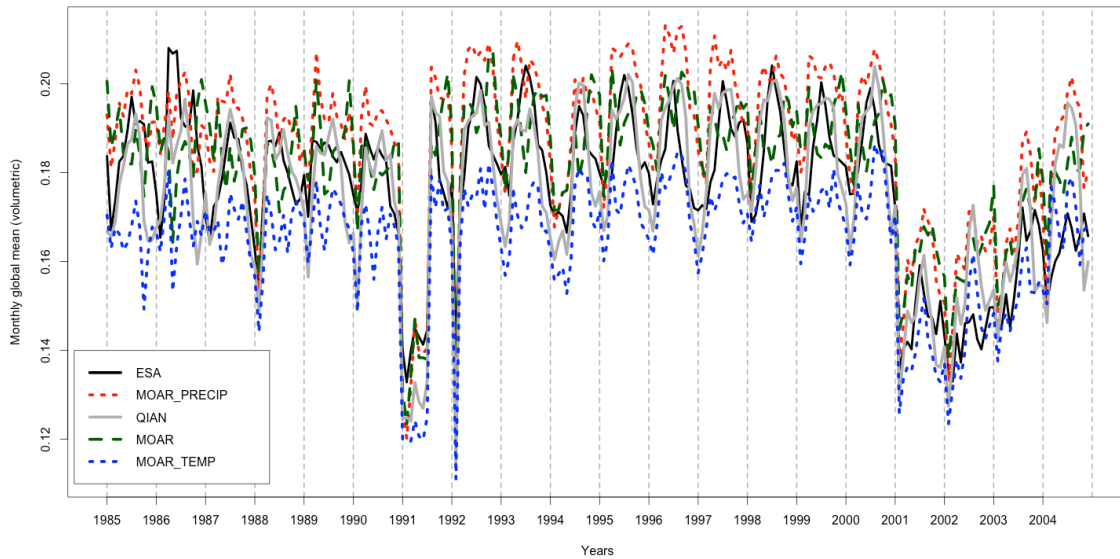


557

558 Figure 7. Global mean monthly runoff (10-year average) of model simulations and
 559 GRDC data indicates that CCSM simulation matched GRDC well April to September.
 560 QIAN simulation matched GRDC in all months but June and July. MOAR_PRECIP run
 561 has high positive biases in the months when MOAR precipitation is more positively
 562 biased than the Qian's reanalysis. MOAR_TEMP run simulation has greater negative
 563 biases throughout the year.

564 The annual cycle of global mean surface soil moisture also demonstrates
 565 hydrological compensation in simulations due to opposing effects of modeled
 566 precipitation and temperature inputs (Figure 8). The 1991 trough is related to a
 567 global precipitation deficiency associated with a warm El Niño Southern
 568 Oscillation (<http://www.isse.ucar.edu/sadc/chptr5.html>). The trough starting in
 569 2001 are the results of the millennium drought in many areas (e.g., [van Dijk et
 570 al., 2013; Wandel et al., 2009]). The ESA data generally have troughs in January
 571 and peaks in the middle of the year (i.e. June and July). The MOAR simulation
 572 tends to have two peaks in the first and second half of a year (e.g., year 1995)
 573 and has more intra-annual variability than the observations. The QIAN simulation
 574 follows the observations more closely in both phase and magnitude, except for
 575 the years after 2002, indicating that sources of uncertainty are more likely from
 576 the atmospheric forcings. Similar as surface runoff, the surface soil moisture
 577 simulations were shifted upwards by MOAR_PRECIP and downwards by
 578 MOAR_TEMP relative to the MOAR run.

579



580
 581 Figure 8. Global mean monthly soil moisture (1985-2004) of model simulations and
 582 observations shows that seasonal moisture dynamics are out of phase in some years
 583 (i.e. opposite wet and dry extremes). Basically all runs except MOAR_TEMP
 584 overestimated runoff globally, implying the deficiency is more likely from land surface
 585 model rather than forcing data.

586 3.5 Potential sources of bias from CLM4

587 If we assume the CLM4 offline run driven by Qian's reanalysis data eliminates
 588 most of the uncertainty generated by atmospheric forcing, the rest of the QIAN
 589 simulation bias is most likely induced by CLM4 itself. The QIAN simulation has
 590 negative runoff bias in the Amazon, central Africa, southwest China, and south
 591 Asia. Comparing with soil texture maps generated by National Aeronautics and
 592 Space Administration Land Data Assimilation Systems
 593 (<http://ldas.gsfc.nasa.gov/gldas/GLDASsoils.php>) and by Global Soil Wetness
 594 Project-Phase 3 ([http://hydro.iis.u-tokyo.ac.jp/~sujan/research/gswp3/soil-texture-](http://hydro.iis.u-tokyo.ac.jp/~sujan/research/gswp3/soil-texture-map.html)
 595 [map.html](http://hydro.iis.u-tokyo.ac.jp/~sujan/research/gswp3/soil-texture-map.html)), the areas with runoff underestimation are mostly associated with high
 596 clay content soils including sandy clay loam, clay loam, and clay. The bias may
 597 be propagated from the mischaracterization of clayey soils though pedo-transfer
 598 functions or parameterizations. For example, clayey soils tend to exhibit
 599 aggregation structure, which is one of most important characteristics of
 600 macropore formation. Macropores enable water to flow through unsaturated soil
 601 more rapidly than it would in a soil matrix defined by Darcy's law [Beven and
 602 Germann, 1982]. The existence of macropores increases effective hydraulic
 603 conductivity, thus decreases water content in surface soils. Without this
 604 mechanism, CLM4 may overestimate evapotranspiration and in turn
 605 underestimate runoff by retaining too much plant available water. Comparing to

606 FLUXNET-MTE global land estimates, *Tang and Riley* [In review] found that
607 CLM4.5 overestimated evapotranspiration in the same areas where runoff was
608 underestimated in this study. We propose that macropore flow is an essential
609 mechanism that is lacking in the CLM and may be responsible for the mis-
610 partitioning of water among evapotranspiration, groundwater, and runoff in
611 tropical and other high clay content areas.

612 Another important process often associated with clayey soils is the shallow
613 subsurface lateral drainage (i.e. interflow) [*McDaniel et al.*, 2008]. The restricting
614 layers formed by argillic and fragipan horizons intercept percolating water and
615 contribute to river discharge directly thus contribute much more rapidly than
616 groundwater [*Jackson et al.*, 2014]. Hillslope with restricting layers may therefore
617 produce considerably more runoff than those without argillic/fragipan layers
618 [*Needelman et al.*, 2004]. The CLM hydrology contains no lateral drainage except
619 in frozen soils. We therefore argue that adding lateral drainage in the high clay
620 content soils with high contrast hydraulic conductivity may potentially change the
621 water balance in the areas currently with large runoff biases. The lateral drainage
622 from restricting layer may be directly added to the surface runoff depending on
623 the topography and river channel network.

624 The areas where runoff simulation is overestimated overlap with the global
625 distribution of Andisols [*Takahashi and Shoji*, 2002]. Defined by United States
626 Department of Agriculture soil taxonomy
627 (http://www.nrcs.usda.gov/Internet/FSE_DOCUMENTS/nrcs142p2_051232.pdf),
628 Andisols are soils formed in volcanic ash with very high porosity (often >0.60
629 $\text{cm}^3 \text{cm}^{-3}$) and therefore high water holding capacity. The mineral soil porosity θ
630 is defined by sand content in CLM as $\theta = 0.489 - 0.00126(\%sand)$. Increasing
631 porosity has been shown to be among the most sensitive parameters for
632 decreasing runoff yield in a physically-based hydrologic model [*Du et al.*, 2013].
633 With low porosity, CLM4 may retain insufficient plant available water and
634 underestimate evapotranspiration, therefore partitioning too much to runoff.
635 Sensitivity of surface hydrology to saturated hydraulic conductivity and porosity
636 needs to be evaluated before future modifications are taken, as the two
637 parameters were identified as secondarily significant to runoff and sensible/latent
638 heat flux after subsurface runoff parameters [*Hou et al.*, 2012; *Huang et al.*,
639 2013]. The proposed modifications are speculated by overlapping the biases with
640 the CLM soil texture map and need further test and proof.

641

642 **4. Summary**

643 Comparisons of surface soil moisture between fully coupled model simulations
644 and observations reveal large positive biases, mostly in mid- to high-latitude
645 areas, except for CCSM4, FGOALS, and BCC. Runoff is overestimated in
646 mountain ranges and in most of the arctic by all CMIP5 models except GISS. All
647 models underestimated runoff in Amazon areas. Terrestrial water storage and
648 dynamics at high northern latitudes are critical to the global water balance.
649 Hydrological fluxes have been poorly monitored in these areas [Kane, 2005], and
650 hydrologic models have difficulties obtaining high quality data for calibration and
651 validation. Current model deficiencies, like those presented above, urge the land
652 modeling community to better understand hydrologic cycles in high latitudes and
653 to help improve overall performance of the models.

654 When assessing runoff and soil moisture, one should not seek an exact match
655 between model simulations and observations due to the mismatch and
656 uncertainty derived from both ends. The validation of soil moisture from land
657 surface modeling should focus mainly on relative changes and dynamics, but we
658 do need to pay attention to the areas consistently having large biases. For
659 example, the CIMP5 archived CLM simulated 10-cm soil moisture was up to 10%
660 different from the observed moisture in 2-5 cm in many areas such as southern
661 China and central/ southern Africa over the long term. The discrepancies were
662 expectedly reduced in the offline tests with 4.5-cm soil moisture and ice content
663 excluded, however the overall spatial pattern was retained. The simulated runoff
664 had the same sign of bias in the same area and implied precipitation might be
665 responsible for the dry or wet in both variables. There were also areas where the
666 biases are opposite sign from soil moisture and runoff such as east half of the
667 United States. It indicates that the land model may not correctly partition the
668 water into surface runoff and infiltration.

669 CCSM4 produces reasonable soil moisture estimates (except where wetlands
670 are included) and positive runoff bias in mountain ranges and central Africa.
671 Negative runoff biases are found mainly in the Amazon, Southeast Asia, and the
672 Middle East. Positive bias of global mean runoff occurred mainly in February-
673 April and October-December. CCSM4 globally averaged surface soil moisture
674 follows observed seasonal cycles but is out of phase compared to ESA data in
675 some years. Overall, CCSM4 produces less bias in surface soil moisture
676 prediction compared to eight other CMIP5 models, but has similar runoff over-
677 predictions in high altitude and high latitude areas as most of the other models.

678 Modeled precipitation and temperature errors generate compensating biases in
679 CCSM4 soil moisture and runoff. Offline CLM4 runs driven by simulated and
680 reanalysis atmospheric inputs reveal that simulated precipitation causes
681 overestimation of runoff in the mountainous areas, east Amazon, and central

682 Africa, and a general increase in overestimation of soil moisture. CLM4 tends to
683 compensate for these overestimations when provided with simulated temperature
684 and humidity, but at the cost of exacerbating surface soil moisture
685 underestimates in high latitudes.

686 Bias from atmosphere forcings is not sufficient to explain all the deviation of
687 simulated runoff and soil moisture from observation. Driven by Qian's reanalysis
688 data, the CLM4 underestimates runoff in Amazon, central Africa, and other areas
689 with high soil clay content. We hypothesize that the lack of fast path water
690 infiltration is partially responsible for erroneous partitioning between
691 evapotranspiration and runoff. CLM does not include preferential fast flow
692 through macropore structure, and implementing this structure into global scale
693 climate model is a challenging task involving extra parameterization and
694 computational demand. Adding lateral drainage within the shallow soil layers is
695 however relatively straightforward, but the model sensitivity needs to be tested
696 first. We also hypothesize that low soil porosity causes overestimation of runoff in
697 mountainous areas with volcanic soils. Improving these processes and data in
698 CLM might help correct the compensating sensitivities of soil moisture and runoff
699 to errors in precipitation and temperature inputs.

700

701 Acknowledgement: This material is based upon work supported by the U.S.
702 Department of Energy, Office of Science, Climate and Environmental Sciences
703 Division, BER Program, under Contract Number DE-AC02-05CH11231.

704

705

706

707

708

709

710

711

712

713

714 **References:**

- 715 Al-Yaari, A., et al. (2014), Global-scale evaluation of two satellite-based passive microwave soil
716 moisture datasets (SMOS and AMSR-E) with respect to Land Data Assimilation System estimates,
717 *Remote Sensing of Environment*, *149*, 181-195.
- 718 Albergel, C., P. de Rosnay, C. Gruhier, J. Munoz-Sabater, S. Hasenauer, L. Isaksen, Y. Kerr, and W.
719 Wagner (2012), Evaluation of remotely sensed and modelled soil moisture products using global
720 ground-based in situ observations, *Remote Sensing of Environment*, *118*, 215-256.
- 721 Albergel, C., W. A. Dorigo, G. Balsamo, J. Munoz-Sabater, P. de Rosnay, L. Isaksen, L. Brocca, R.
722 de Jeu, and W. Wagner (2013), Monitoring multi-decadal satellite earth observation of soil
723 moisture products through land surface reanalyses, *Remote Sensing of Environment*, *138*, 77-89,
724 doi:10.1016/j.rse.2013.07.009.
- 725 Alkama, R., L. Marchand, A. Ribes, and B. Decharme (2013), Detection of global runoff changes:
726 results from observations and CMIP5 experiments, *Hydrology and Earth System Science*, *10*,
727 2117-2140, doi:10.5194/hessd-10-2117-2013.
- 728 Becker, A., P. Finger, A. Meyer-Christoffer, B. Rudolf, K. Schamm, U. Schneider, and M. Ziese
729 (2013), A description of the global land-surface precipitation data products of the Global
730 Precipitation Climatology Centre with sample applications including centennial (trend) analysis
731 from 1901-present, *Earth System Science Data*, *5*, 71-99, doi:10.5194/essd-5-71-2013.
- 732 Beven, K., and P. Germann (1982), Macropores and water flow in soils, *Water Resources*
733 *Research*, *18*(5), 1311-1325.
- 734 Brocca, L., et al. (2011), Soil moisture estimation through ASCAT and AMSR-E sensors: an
735 intercomparison and validation study across Europe, *Remote Sensing of Environment*, *115*, 3390-
736 3408.
- 737 Collins, W. D., et al. (2006), The Community Climate System Model Version 3 (CCSM3), *Journal of*
738 *Climate*, *19*, 2122-2143.
- 739 Collins, W. D., et al. (2014), The integrated Earth System Model (iESM): Formulation and
740 functionality, *GeoSi. Model Dev. Discuss*, in review.
- 741 Dai, A., T. Qian, and K. E. Trenberth (2009), Changes in continental freshwater discharge from
742 1948 to 2004, *Journal of Climate*, *22*, 2773-2791.
- 743 Decker, M., and X. Zeng (2009), Impact of modified Richards equation on global soil moisture
744 simulation in the Community Land Model (CLM3.5), *Journal of Advances in Modeling Earth*
745 *Systems*, *1*, 22, doi:10.3894/JAMES.2009.1.5.
- 746 Di Vittorio, A. V., et al. (2014), From land use to land cover: restoring the afforestation signal in a
747 coupled integrated assessment–earth system model and the implications for CMIP5 RCP
748 simulations, *Biogeosciences*, *11*, 6435-6450, doi:10.5194/bg-11-6435-2014.
- 749 Dorigo, W. A., et al. (2014), Evaluation of the ESA CCI soil moisture product using ground-based
750 observations, *Remote Sensing of Environment*, doi:<http://dx.doi.org/10.1016/j.rse.2014.07.023>.
- 751 Du, E., T. E. Link, J. A. Gravelle, and J. A. Hubbart (2013), Validation and sensitivity test of the
752 distributed hydrology soil-vegetation model (DHSVM) in a forested mountain watershed,
753 *Hydrological Processes*, doi:10.1002/hyp.10110.
- 754 Fekete, B. M., and C. J. Vorosmarty (2002), High-resolution fields of global runoff combining
755 observed river discharge and simulated water balances, *Global Biogeochemical Cycles*, *16*(3),
756 doi:10.1029/1999GB001254.
- 757 Field, C. B., et al. (2014), IPCC, 2014: Climate Change 2014: Impacts, Adaptation, and
758 Vulnerability. Part A: Global and Sectoral Aspects. Contribution of Working Group II to the Fifth
759 Assessment Report of the Intergovernmental Panel on Climate Change *Rep.*, 1132 pp pp,
760 Cambridge, United Kingdom and New York, NY, USA.

761 Gedney, N., P. M. Cox, R. A. Betts, O. Boucher, O. Huntingford, and P. A. Stott (2006), Detection
762 of a direct carbon dioxide effect in continental river runoff records, *Nature*, *439*, 835-838.
763 Gerten, D., S. Rost, W. von Bloh, and W. Lucht (2008), Causes of change in 20th century global
764 river discharge, *Geophysical Research Letters*, *35*, doi:1029/2008GL035258.
765 Gruhier, C., et al. (2010), Soil moisture active and passive microwave products: intercomparison
766 and evaluation over a Sahelian site, *Hydrology and Earth System Science*, *14*, 141-156.
767 Hou, Z., M. Huang, L. R. Leung, G. Lin, and D. M. Ricciuto (2012), Sensitivity of surface flux
768 simulations to hydrologic parameters based on an uncertainty quantification framework applied
769 to the Community Land Model, *Journal of Geophysical Research*, *117*, D15108,
770 doi:10.1029/2012JD017521, 2012.
771 Huang, M., Z. Hou, L. R. Leung, Y. Ke, Y. Liu, Z. Fang, and Y. Sun (2013), Uncertainty of runoff
772 simulaitons and parameter identifiability in the Community Land Model: evidence from MOPEX
773 basins, *Jounral of Hydrometeorology*, *14*, 1754, doi:10.1175/JHM-D-12-0138.1.
774 Jackson, C. R., M. Bitew, and E. Du (2014), When interflow also percolates: downslope travel
775 distances and hillslope process zones, *Hydrological Processes*, *28*, 3195-3200,
776 doi:10.1002/hyp.10158.
777 Kane, D. L. (2005), High-latitude hydrology, what do we know?, *Hydrological Processes*, *19*,
778 2453-2454, doi:10.1002/hyp.5929.
779 Labat, D., Y. G. Aeris, and J. L. Guyot (2004), Evidence for global runoff increase related to
780 climate warming, *Advances in Water Resources*, *27*, 631-642.
781 Lawrence, D. M., et al. (2011), Parameterization improvements and functional and structural
782 advances in Version 4 of the Community Land Model, *Journal of Advances in Modeling Earth
783 System*, *3*, 27, doi:10.1029/2011MS000045.
784 Liu, Y. Y., W. A. Dorigo, R. M. Parinussa, R. A. M. de Jeu, W. Wagner, M. F. McCabe, J. P. Evans,
785 and A. I. J. M. van Dijk (2012), Trend-preserving blending of passive and active microwave soil
786 moisture retrievals, *Remote Sensing of Environment*, *123*, 280-297,
787 doi:10.1016/j.rse.2012.03.014.
788 Loew, A., T. Stacke, W. A. Dorigo, R. A. M. de Jeu, and S. Hagemann (2013), Potential and
789 limitations of multidecadal satellite soil moisture observations for selected climate model
790 evaluation studies, *Hydrology and Earth System Science*, *17*, 3523-3542, doi:10.5194/hess-17-
791 3523-2013.
792 Luo, Y. Q., et al. (2012), A framework for bencharking land models, *Biogeosciences*, *9*, 3857-3874,
793 doi:10.5194/bg-9-3857-2012.
794 McCabe, G. J., and D. M. Wolock (2011), Century-scale variability in global annual runoff
795 examined using a water balance model, *International Journal of Climatology*, *31*, 1739-1748,
796 doi:10.1002/joc.2198.
797 McDaniel, P. A., M. P. Regan, E. Brooks, J. Boll, S. Barndt, A. Falen, S. K. Young, and J. E. Hammel
798 (2008), Linking fragipans, perched water tables, and catchment-scale hydrological processes,
799 *Catena*, *73*, 166-173, doi:10.1016/j.catena.2007.05.011.
800 Mehran, A., A. AghaKouchak, and T. J. Philips (2014), Evaluation of CMIP5 continental
801 precipitation simulations relative to satellite-based gauge-adjusted observations, *Jounral of
802 Geophysical Research*, *35*, doi:doi: 10.1002/2013JD021152.
803 Needelman, B. A., W. J. Gburek, G. W. Petersen, A. N. Sharpley, and P. J. Kleinman (2004),
804 Surface runoff along two agricultural hillslopes with contrasting soils, *Soil Science Socieity of
805 America*, *68*, 914-923.
806 Niu, G. Y., R. E. Dickinson, and L. E. Gulden (2005), A simple TOPMODEL-based runoff
807 parameterization (SIMTOP) for use in global climate models, *Journal of Geophysical Research*,
808 *110*(D21106), doi:10.1029/2005JD006111.

809 Niu, G. Y., Z. L. Yang, R. E. Dickinson, L. E. Gulden, and H. Su (2007), Development of a simple
810 groundwater model for use in climate models and evaluation with Gravity Recovery and Climate
811 Experiment data, *Journal of Geophysical Research*, *112*, doi:10.1029/2006JD007522.

812 Oleson, K. W., et al. (2010), Technical description of version 4.0 of the Community Land Model
813 (CLM).*Rep.*, 257 pp, NCAR Tech. Note NCAR/TN-4781STR.

814 Oleson, K. W., et al. (2008), Improvements to the Community Land Model and their impact on
815 the hydrological cycle, *Journal of Geophysical Research*, *113*, doi:10.1029/2007JG000563.

816 Owe, M., R. de Jeu, and T. Holmes (2008), Multisensor historical climatology of satellite-derived
817 global land surface moisture, *Journal of Geophysical Research*, *113*, doi:10.1029/2007JF000769,
818 2008.

819 Piao, S., P. Friedlingstein, P. Ciais, N. de Noblet-Ducoudre, D. Labat, and S. Zaehle (2007),
820 Changes in climate and land use have a larger direct impact than rising CO₂ on global river runoff
821 trends, *Proceedings of the National Academy of Sciences*, *104*, 15242-15247.

822 Qian, T., A. Dai, K. E. Trenberth, and K. W. Oleson (2006), Simulation of global land surface
823 conditions from 1948 to 2004. Part I: forcing data and evaluations, *Journal of Hydrometeorology*,
824 *7*, 23.

825 Schneider, U., A. Becker, P. Finger, A. Meyer-Christoffer, B. Rudolf, and M. Ziese (2011), GPCP
826 full data reanalysis version 6.0 at 1.0°: monthly land-surface precipitation from rain-gauges built
827 on GTS-based and historic data, edited by G. P. C. Centre, Boulder, Colorado USA,
828 doi:10.5676/DWD_GPCP/FD_M_V6_100.

829 Seneviratne, S. I., et al. (2013), Impact of soil-climate feedbacks on CMIP5 projections: first
830 results from the GLACE-CMIP5 experiment, *Geophysical Research Letters*, *40*, 5212-5217,
831 doi:10.1002/grl.50956, 2013.

832 Shi, X., J. Mao, P. E. Thornton, F. M. Hoffman, and W. M. Post (2011), The impact of climate, CO₂,
833 nitrogen deposition and land use change on simulated contemporary global river flow,
834 *Geophysical Research Letters*, *38*, doi:10.1029/2011GL046773.

835 Takahashi, T., and S. Shoji (2002), Distribution and classification of volcanic ash soils, *Global*
836 *Environmental Research*, *6*(2), 83-97.

837 Tang, J., and W. J. Riley (In review), Impacts of incorporating root hydraulic redistribution on
838 global evapotranspiration, edited.

839 Taylor, K. E., R. J. Stouffer, and G. A. Meehl (2012), An overview of CMIP5 and the experiment
840 design, *American Meteorological Society*, 485-498, doi:10.1175/BAMS-D-11-00094.1.

841 van Dijk, A. I. J. M., H. E. Beck, R. S. Crosbie, R. A. M. de Jeu, Y. Y. Liu, G. M. Podger, B. Timbal,
842 and N. R. Viney (2013), The Millennium Drought in southeast Australia (2001–2009): Natural and
843 human causes and implications for water resources, ecosystems, economy, and society, *Water*
844 *Resources Research*, *49*, 1-18, doi:10.1029/2013WR017233; DOI: 10.1002/wrcr.20123.

845 Wagner, W., G. Lemoine, and H. Rott (1999), A method for estimating soil moisture from ERS
846 scatterometer and soil data, *Remote Sensing of Environment*, *70*, 191-207.

847 Wandel, J., G. Young, and B. Smit (2009), The 2001-2001 drought: vulnerability and adaptation in
848 Alberta's special areas, *Prairie Forum*, *34*(1), 211-234.

849

850